Applicability of the Morison equation for calculating loads on a vertical cylinder due to breaking and near-breaking waves

E. Buldakov

Department of Civil Engineering, UCL, Gower Street, LONDON, WC1E 6BT, UK
email: e.buldakov@ucl.ac.uk

1 Introduction

The Morison equation (Morison et al. 1950) provides a simple method of estimating wave loads on structures, which remains among methods recommended by design codes (e.g. DNV 2019). The equation uses undisturbed wave kinematics and assumes that the flow around a structure is almost uniform. This implies a slender body approximation when the wave length is much larger than the structure diameter. Rainey (1995) suggested additional terms to extend the applicability of the slender body approximation. Chaplin et al. (1997) applied different combinations of classical Morison and additional terms to calculate the load on a vertical cylinder in the inertia regime in steep non-breaking wave groups. They used regular wave kinematics based on stream function solutions and wave group kinematics computed using a fully non-linear potential flow theory. Best results were achieved by using the Morison inertia term, 'axial divergence force' and 'surface intersection force' in combination with FNPF wave group kinematics. However, near-breaking and breaking waves exhibit significant non-uniformity near the crest, as can be seen in Fig. 1a and Fig. 2a. This raises questions about the applicability of a slender-body approach. For interaction with sharp crests of high waves simple slamming models are used. For instance, for a vertical slender cylinder, DNV (2019) recommends employing a strip-wise approach. Each section is treated as a 2D cylinder entering an infinite water body, with the impact load calculated using an empirical slamming coefficient. The assumptions involved are clearly not valid for flows like those shown in Fig. 1a as the compact wave crest can be easily distorted by the cylinder. This paper attempts to resolve the issues described above.

2 Experiments and incoming wave kinematics

For test cases we use experiments conducted by Esandi et al. (2020), who studied the interaction of spilling breaking and near-breaking waves with a fixed truncated vertical cylinder (Fig. 1a). The wave groups with a Gaussian amplitude spectrum were generated in 1 m deep water and focussed at a position 11 m from the wavemakers, aligning with the front of the cylinder. The cylinder, with a diameter of 165 mm, had a draught of 0.8 m in still water. The main natural frequency of the installation was 6.5 Hz. We focus on three wave cases with a spectral peak period of $T_p = 1.4\,\text{sec}$ and linear focussed amplitudes of $A_f = 13.5\,\text{cm}$, $13.95\,\text{cm}$ and $14.4\,\text{cm}$, representing high non-breaking, weakly-breaking and strong-breaking conditions (T14NB3, T14BR1 and T14BR2). We use linear wave characteristics for the peak spectral frequency to calculate non-dimensional parameters. The value of the ratio of the wave length to cylinder diameter $\lambda/D = 18$ formally justifies the application of the slender body approximation and the Keulegan-Carpenter numbers $KC \approx 5.3$, 5.5 and 5.7 are just outside the accepted inertia flow regime.

Incoming wave kinematics in this study is obtained using a Numerical Wave Tank based on a 2D Lagrangian numerical wave model with breaking dissipation (Buldakov 2021). The model describes the temporal evolution of fluid particle coordinates $x = x(a, c, t)$; $z = z(a, c, t)$ fixed in Lagrangian space (a, c). When using Lagrangian kinematics with the Morison equation, we transfer fluid properties between Lagrangian to Eulerian spaces as needed. We replicate the experimental wave tank in the numerical model by implementing appropriate boundary conditions. A flap wavemaker is simulated at one end of the tank and the waves are absorbed by a dissipative region at the other end. The motion of the wavemaker recorded in the experiment is used as the model input and other model parameters are selected through a convergence study.

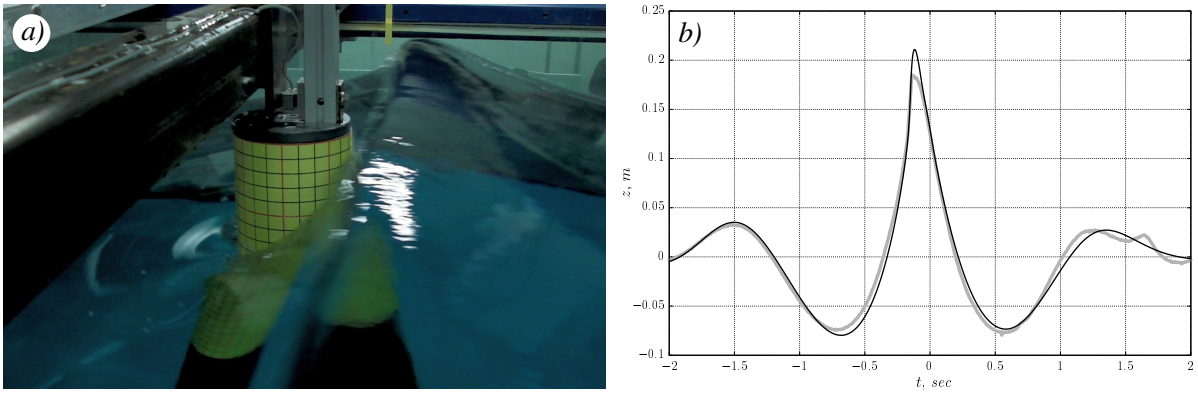

Figure 1: a) Wave interaction with a cylinder prior to crest impact in the wave flume experiment. Case T14BR2. b) Time history of surface elevation of an incoming wave at the cylinder front ($x = 11\,\mathrm{m}$). Grey – experiment; black – numerical Lagrangian wave tank. Case T14BR2.

Comparison of time history of surface elevation of an incoming wave at the focus location can be seen in Fig. 1b.

3 Load calculation

We experimented with different term combinations for load calculation, including classical Morison drag and inertia terms based on centreline kinematics and Froude-Krylov force. All of them failed near high peaks, resulting in substantial load overestimation. The most accurate results were achieved using the calculation method described below.

We calculate the horizontal inertia force F_I and the corresponding moment by using the following generalised form of the inertia term of the Morison equation, which accounts for the changing displacement volume and the non-uniformity of the flow field

$$F_I = \rho\, C_M \int\limits_{V_D(t)} a_x\, dV; \qquad M_I = \rho\, C_M \int\limits_{V_D(t)} (Z_c - z)\, a_x\, dV, \tag{1}$$

where $a_x = \ddot{x}(a, c, t)$ is the material acceleration in the horizontal direction, the inertial coefficient C_M is set to 2 and the integral is taken over the volume V_D displaced by the cylinder below the wave surface. Note, that the integration volume changes over time and integrals in this paper are taken in Eulerian space. The moment of force is calculated relative to the mounting centre of the model with the distance from the still water level $Z_c = 345\,\mathrm{mm}$. Results of application of (1) are illustrated in Fig. 3. The calculated load compares well to experiment, with the exception of a small vicinity of the crest where the additional loads due to impact and significant crest deformation are not captured by the inertia term (1).

To consider the interaction of the cylinder with a high wave crest, we first introduce the crest distortion volume V_{CD} and the crest impact area S_{CI} (Fig. 2b). The volume is limited by part of the wave surface BC, the horizontal plane AC and part of the cylinder surface AB, which is treated as the impact area. Only the part of the crest above AC contributes to the load and only positive horizontal velocity and positive load are taken into account. To calculate the impact load, we consider the change in fluid momentum normal to the cylinder surface. It is assumed that the tangential momentum is preserved. For a non-elastic impact, the normal momentum disappears, while for a perfectly elastic impact (splashing), the normal momentum changes sign. Then the impact load can be calculated as

$$F_{CI} = \rho\, C_I \int\limits_{S_{CI}(t)} u_n^2\, n_x\, dS\,; \qquad M_{CI} = \rho\, C_I \int\limits_{S_{CI}(t)} (Z_c - z)\, u_n^2\, n_x\, dS\,, \tag{2}$$

where u_n is the velocity component normal to the cylinder surface and n_x is the x-component of an unit inner normal vector. For a vertical circular cylinder they can be calculated as

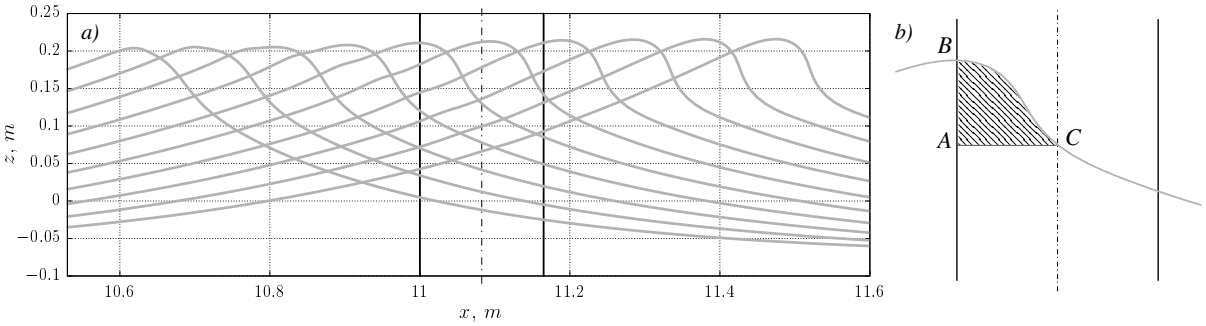

Figure 2: a) Wave crest evolution of a simulated undisturbed wave in the vicinity of the cylinder. Case T14BR2. Snapshots of surface elevation profiles are taken from $t = -0.32\,\text{sec}$ to $t = 0.13\,\text{sec}$ with a time step $\Delta t = 0.05\,\text{sec}$. b) Definition of impact area and volume for crest impact model.

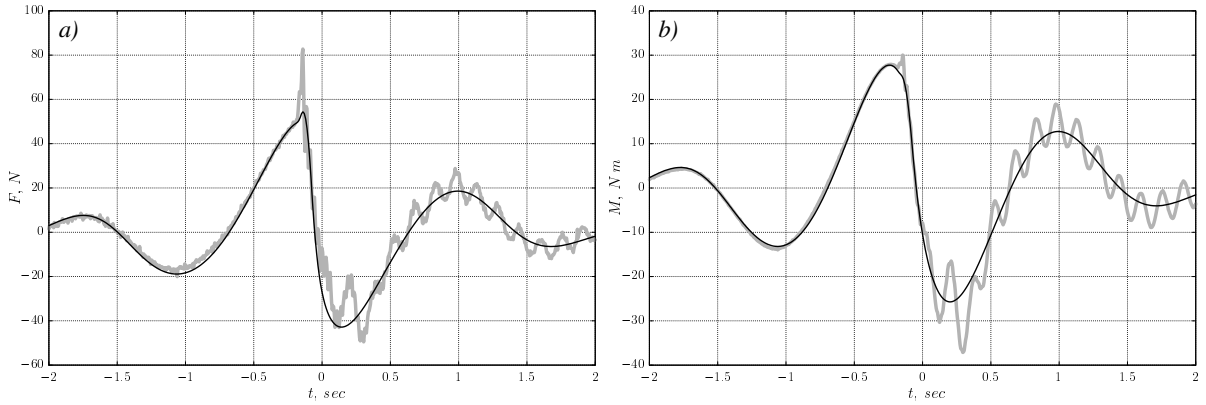

Figure 3: Wave load on the cylinder for case T14BR2. Grey – experiment, black – numerical evaluation using the inertia term (1). a) Horizontal force. b) Moment of force relative to a model mounting centre 345 mm above the still water level.

$u_n = \dot{x}(a, c, t)\cos\alpha$ and $n_x = \cos\alpha$, α being the angle from the front of the cylinder in a horizontal plane. The impact coefficient C_I is equal to 1 for a non-elastic impact and 2 for a perfectly elastic one. We determine the crest distortion force and moment as the rate of change of momentum and angular momentum in the varying crest distortion volume $V_{CD}(t)$ defined above. We have

$$F_{CD} = \rho \frac{d}{dt} \int\limits_{V_{CD}(t)} u \, dV; \qquad M_{CD} = \rho \frac{d}{dt} \int\limits_{V_{CD}(t)} (Z_c - z)\, u \, dV\,, \tag{3}$$

where $u = \dot{x}(a, c, t)$ is the horizontal fluid velocity.

4 Results

The comparison of calculated peak loads with experiments is presented in Fig. 4. It can be observed that for a non-breaking wave (Fig. 4a) the best result is demonstrated by a combination of the inertia term (1) with the crest distortion term (3). In the case of breaking waves (Fig. 4b, c), the addition of the impact term (2) with $C_{CI} = 2$ is necessary, describing the splashing impact. It is suggested that for weaker breaking $C_{CI} = 1$ corresponding to an inelastic impact may be appropriate. The overall comparison is good when the correct combination of terms is selected. Further improvements can be achieved by including the structural response and secondary loading cycle (Chaplin et al. 1997).

References

Buldakov, E. (2021), Wave propagation models for numerical wave tanks, *in* D. M. Kelly, A. Dimakopoulos & P. Higuera, eds, 'Advanced Numerical Modelling of Wave Structure Interaction', CRC Press, pp. 36–68.

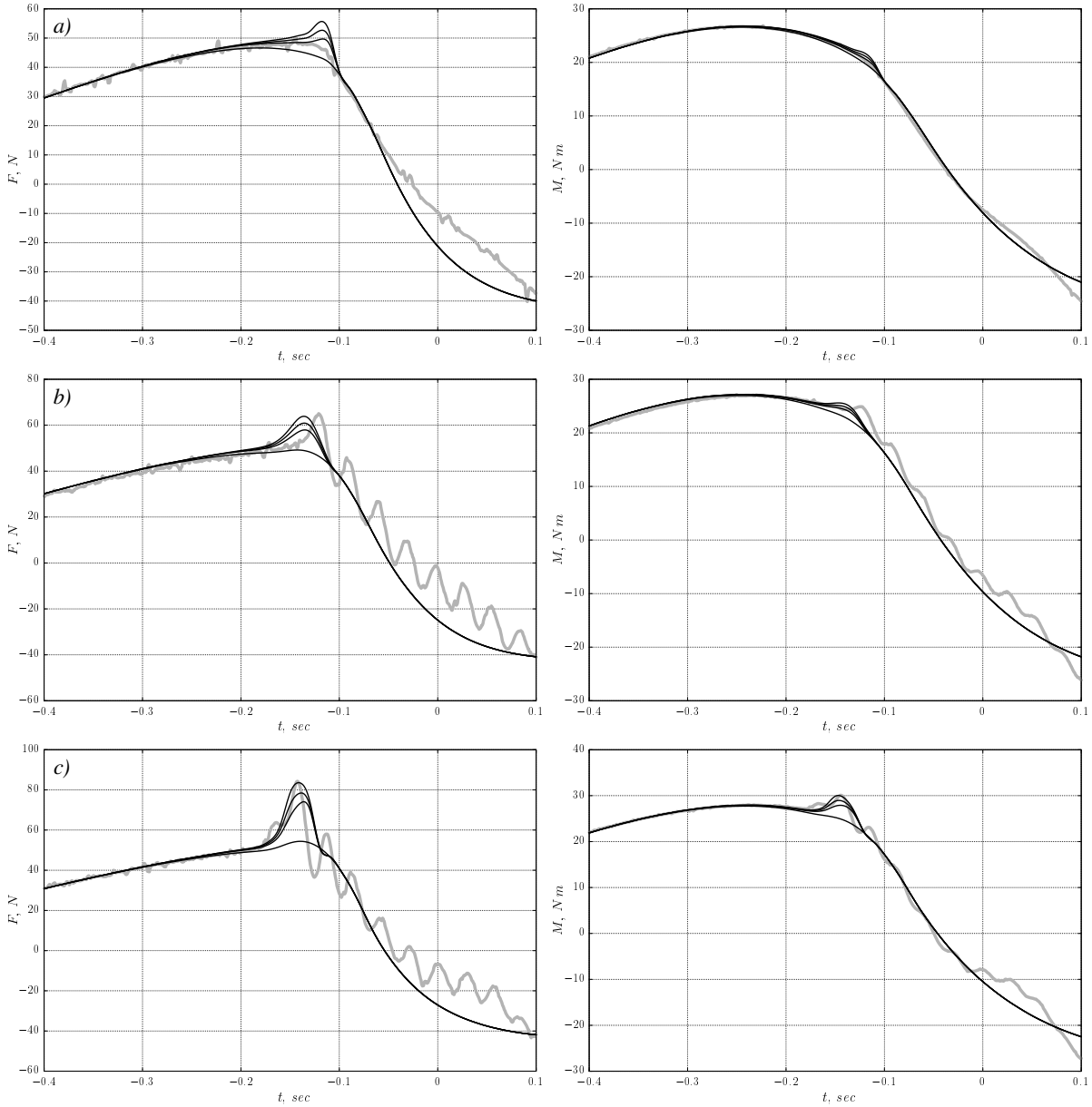

Figure 4: Wave loads on the cylinder around crest impact. Left – horizontal force, right – moment of force relative to a model mounting centre. Grey – experiment, black – numerical evaluations using various combinations of components in order of increasing load: inertia term (1), plus crest distortion term (3), plus impact term with $C_I = 1$ and $C_I = 2$ (2). a) Case T14NB3; b) Case T14BR1; c) Case T14BR2.

Chaplin, J. R., Rainey, R. C. T. & Yemm, R. W. (1997), 'Ringing of a vertical cylinder in waves', *Journal of Fluid Mechanics* **350**, 119147.

DNV (2019), *DNV-RP-C205: Environmental conditions and environmental loads*, DNV AS.

Esandi, J. M., Buldakov, E., Simons, R. & Stagonas, D. (2020), 'An experimental study on wave forces on a vertical cylinder due to spilling breaking and near-breaking wave groups', *Coastal Engineering* **162**, 103778.

Morison, J., Johnson, J. & Schaaf, S. (1950), 'The Force Exerted by Surface Waves on Piles', *Journal of Petroleum Technology* **2**(05), 149–154.

Rainey, R. (1995), 'Slender-body expressions for the wave load on offshore structures', *Proceedings - Royal Society of London, A* **450**(1939), 391 416.